IRIS AperTO

UNIVERSITÀ DEGLI STUDI DI TORINO

AperTO - Archivio Istituzionale Open Access dell'Università di Torino

Blue fluorescent zinc(II) complexes based on tunable imidazo[1,5-a]pyridines

This is the author's manuscript

Original Citation:

Availability:

This version is available http://hdl.handle.net/2318/1765795 since 2021-10-26T15:01:48Z

Published version:

DOI:10.1016/j.ica.2020.119662

Terms of use:

Open Access

Anyone can freely access the full text of works made available as "Open Access". Works made available under a Creative Commons license can be used according to the terms and conditions of said license. Use of all other works requires consent of the right holder (author or publisher) if not exempted from copyright protection by the applicable law.

(Article begins on next page)

13 December 2025

IRIS AperTO

UNIVERSITÀ DEGLI STUDI DI TORINO

This is the author's final version of the contribution published as:

Giorgio Volpi, Emanuele Priola, Claudio Garino, Andrea Daolio, Roberto Rabezzana, Paola Benzi, Alessia Giordana, Eliano Diana, Roberto Gobetto.

Blue fluorescent zinc(II) complexes based on tunable imidazo[1,5-*a*]pyridines

Inorganica Chimica Acta, 509, 2020, 119662.

DOI: 10.1016/j.ica.2020.119662

The publisher's version is available at:
https://www.sciencedirect.com/science/article/pii/S0020169320304825?via%3Dihub

When citing, please refer to the published version.

Link to this full text:
http://hdl.handle.net/2318/1765795

This full text was downloaded from iris-Aperto: https://iris.unito.it/

iris-AperTO

University of Turin's Institutional Research Information System and Open Access Institutional Repository

Blue fluorescent zinc(II) complexes based on tunable imidazo[1,5-*a*]pyridines

Giorgio Volpi,[‡]* Emanuele Priola,[‡] Claudio Garino,* Andrea Daolio, Roberto Rabezzana, Paola Benzi, Alessia Giordana, Eliano Diana and Roberto Gobetto

Department of Chemistry, NIS Interdepartmental Centre, University of Torino, Via Pietro Giuria 7, 10125, Torino, Italy
[‡] These authors contributed equally to this work
Keywords: imidazo[1,5-*a*]pyridine, luminescence, zinc complex, quantum yield, Stokes shift, tunable emission.

Abstract

Herein, we investigate the photophysical features of new zinc(II) chlorido complexes containing fluorescent 1,3-substituted imidazo[1,5-*a*]pyridines as ligands. The derivatives introduce electron-donating or electron-withdrawing moieties in position 3 on the ligand skeleton. The obtained compounds have been characterized with different spectroscopic techniques, their structure has been defined by single-crystal X-ray diffraction and mass spectrometry and their optical properties have been discussed in relation to the chemical structure. The comparison between the emission spectra of the free ligands and of the corresponding zinc(II) chlorido complexes shows an intense hypsochromic shift, due to the modification of the ligands conformation upon metal coordination, and a significant increase of the quantum yield after complexation.

1. Introduction

The demand for optically efficient materials prompts researchers to design new fluorescent organic compounds and luminescent metal derivatives. Their investigation is driven by the necessity to control the chemical structure, the excited states and the photophysical behavior of the new molecules. At this regard, coinage metal derivatives show a great potential, due to their tunable optical properties and high luminescent performances.[1–3] In particular, low-cost coinage metals (such as Cu, Zn, Fe and Al) are becoming the focus of an increasingly widespread field of research,[3–12] in comparison with the most investigated and applied heavy second- or third-row transition metals (such as Au, Pt, Ir, Ru or Re).[13–20]

Recently, zinc(II) complexes have been reported as rising electroluminescent materials for organic light-emitting diodes (OLEDs) and light-emitting electrochemical cells (LECs).[10,11,21] Indeed, the optical behavior of zinc compounds, as emitters, is comparable with that of tris(8-hydroxyquinolinato)aluminium (Alq3), a well know component of organic light-emitting diodes (OLEDs).[11,22] In general, zinc(II) compounds may be important and convenient candidates to improve the performances of optoelectronic devices as luminescent molecule in doped polymer films or as fluorescence emitting dopants.

Herein, we report a study on the synthesis and optical characterization of three new blue luminescent zinc(II) chlorido complexes based on 1,3-substituted-imidazo[1,5-*a*]pyridine ligands (Figure 1), which contain both electron-donating and electron-withdrawing chemical groups. Fluorescent imidazo[1,5-*a*]pyridine derivatives have been employed for many applications, principally as bidentate ligands[23–28] and intense emitters.[29–41] In addition, they have been investigated for biological applications[42–46] and for a wide range of potential pharmaceutical applications.[47–51] In particular, the ligands employed in this work were originally developed to form luminescent Re and Ir complexes[52–54] and to investigate the relationship between chemical structure and electronic properties in ligands containing electron-donating or electron-withdrawing moieties in their skeleton. In the present work, these ligands are combined with zinc(II), to improve their optical behavior towards promising and useful technological applications, in agreement with the recent interest addressed to the luminescent and inexpensive coinage metal derivatives. In order to increase the optical properties, the choice of the ancillary chlorido ligands was based on a previous study concerning the effect of the halides on similar complexes.[7] The main properties of the obtained complexes include: high emission quantum yields and a remarkable blue-shift, opposite to what generally reported for similar compounds, making these compounds unique among the zinc(II) complexes reported so far.

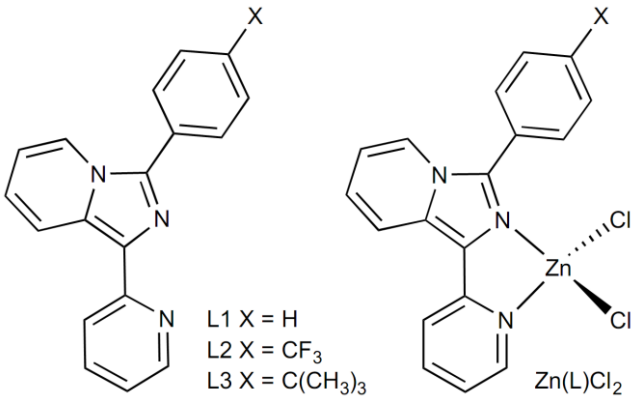

Figure 1. Imidazo[1,5-*a*]pyridine ligands and corresponding Zn(II) complexes $Zn(L)Cl_2$.

2. Results and discussion

2.1. Synthesis

The ligands **L1**, **L2** and **L3** were obtained as previously reported, by a direct one-pot cyclization synthetic approach condensing di(2-pyridyl)ketone with benzaldehyde (**L1**), 4-(trifluoromethyl)benzaldehyde (**L2**) or 4-*tert*-butylbenzaldehyde (**L3**) in acetic acid and ammonium acetate.[27,52–54] Their purity was assessed by TLC, ^{1}H and ^{13}C NMR spectroscopy.
The Zn(II) complexes **Zn(L1)Cl$_2$**, **Zn(L2)Cl$_2$** and **Zn(L3)Cl$_2$** were prepared by reaction of $ZnCl_2$ with 1 equiv. of the corresponding ligand in methanol at room temperature. All the complexes are yellow crystalline powders and were characterized by elemental analysis, mass spectrometry, infrared, UV-visible and emission spectroscopy and single crystal X-ray diffraction. Due to the extremely low solubility of the complexes in the common deuterated solvents, it was not possible to perform their NMR characterization.

2.2 Structural characterization and topological-energetic packing analysis

Zn(L1)Cl$_2$, **Zn(L2)Cl$_2$** and **Zn(L3)Cl$_2$** were successfully crystallized and their crystals investigated by means of single crystal X-ray diffraction. The crystals were obtained by solvent diffusion of a solution of the related ligand into a solution of $ZnCl_2$.

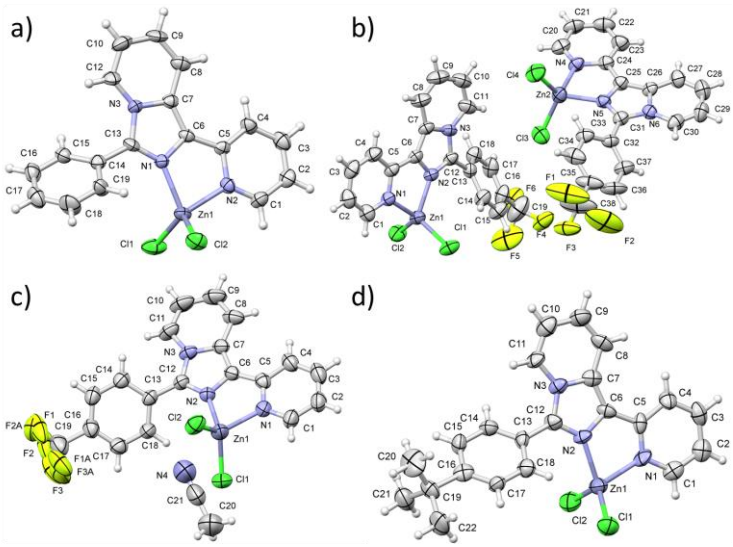

Figure 2. ORTEP diagrams and numeration of asymmetric units of **Zn(L1)Cl$_2$** (a), **Zn(L2)Cl$_2$** form-a (b), **Zn(L2)Cl$_2$** form-b (c) and **Zn(L3)Cl$_2$** (d), thermal ellipsoids drawn at 50% of probability.

Adding a dichloromethane solution of **L1** to a methanolic solution of $ZnCl_2$ the formation of several colorless platelets of **Zn(L1)Cl$_2$** was observed after a day. This zinc complex crystallizes in the monoclinic centrosymmetric *P2$_1$/c* space group and the asymmetric unit is formed by a single molecule (Figure 2a).
Considering the para-substituted derivatives, the trifluoromethane derivative **Zn(L2)Cl$_2$** crystallizes in two different solvate forms. Form-a was obtained adding a methanolic solution of $ZnCl_2$ to a dichloromethane solution of **L2** (Figure 2b), while using an acetonitrile solution of the ligand led to form-b (Figure 2c). The inclusion of the crystallization solvent in these crystals changes noticeably the packing characteristics, although there are no evident changes in the molecular conformation.

With dichloromethane, **Zn(L2)Cl$_2$** crystallizes (form-a) in the monoclinic centrosymmetric *P2$_1$/n* space group with two units of complex and one disordered solvent molecule included in the asymmetric unit (Z' = 3). The two molecules adopt almost the same geometry, and the absence of crystallographic equivalence can be explained with crystal growth effects and with the difference in surrounding interactions.[55] On the other hand, form-b shows triclinic *P-1* symmetry, a single molecule of **Zn(L2)Cl$_2$** in the asymmetric unit and is dominated by π···π stacking between inverted molecules. **Zn(L3)Cl$_2$** was crystallized by adding a solution of **L3** in diethyl ether to an acetonitrile solution of $ZnCl_2$. The complex adopts the triclinic *P-1* space group, with one molecule in the asymmetric unit (Figure 2d).

In all the four structures obtained, the Zn(II) coordination polyhedron is a distorted tetrahedron with two chloride and two nitrogen coordination sites (τ_4= 0.88 for **Zn(L1)Cl$_2$**, 0.94 and 0.88 for the two molecules of **Zn(L2)Cl$_2$** form-a, 0.87 for **Zn(L2)Cl$_2$** form-b and 0.87 for **Zn(L3)Cl$_2$**, according to the definition of Houser and coworkers[56]). In **Zn(L1)Cl$_2$**, the ligand is almost planar, with the phenyl substituent turned around the C13–C14 inter-ring bond by 49.16(10)°. This value is similar or higher to those obtained for the two para-substituted compounds, varying from 41.02(7)° for **Zn(L3)Cl$_2$** to 35.34(8)° in the case of **Zn(L2)Cl$_2$** (form-a and form-b). These values are much lower than those obtained by Ardizzoia and others for Zn(II) complexes containing meta substituted imidazo[1,5-*a*]pyridines,[7] thus demonstrating the possibility of unsubstituted and para-substituted complexes to freely rotate around the intra-ring bond and the relation of this dihedral angle only to steric or packing effects.

Considering the weak interactions that influence the packing environment of **Zn(L1)Cl$_2$**, directional C–H···Cl contacts forming a 2D pattern are present (Figure 3a, see Table S3 for distance values). These interactions are evident in the representation of the shape index projected on the Hirshfeld surface: for the rapid color change in the chlorine region, in the electron density modification around some of the aromatic C–H fragments and in the derived fingerprint for the clear stripes (Figure 3b). Between these planes, the molecules interact each other through π···π interactions, as confirmed by red and blue triangles in the shape index representation (Figure 3c).

In the case of **Zn(L2)Cl$_2$** (form-a), the two Hirshfeld surfaces (Figures S7 and S9) highlight a stronger C–H···Cl interaction for molecule 1 with respect to molecule 2 (this can be appreciated looking the longer and narrower stripes in the fingerprints, Figure S8c and Figure S10c) and a modification in the donor-acceptor ratio for the C–H···F interaction component. Considering the other contacts (Figure S8 and Figure S10), it is worth noting some difference in the π···π stacking: in the packing geometry of the crystal, in which coplanar inverted dimers are present and, perpendicular to those clusters, the second molecule is inserted forming layers of organic matter separated by fluorine and chlorine (Figure 4a). Solvent molecules are inserted in the interlayer without any strong directional interaction.

On the other hand, form-b shows triclinic *P-1* symmetry, a single molecule of **Zn(L2)Cl$_2$** in the asymmetric unit and is dominated by π···π stacking between inverted molecules. Looking at Figure 4b, it is possible to observe the formation of diagonal columns of parallel molecules (with an average interplanar distance of 4.1 Å, but with intermolecular C–H···π distance as short as 2.919(10) Å), shifted by the presence of trifluoromethane substituents and the insertion of acetonitrile molecules. These columns are laterally connected to form layers, separated by a region of only dispersive interactions, in the (100) plane. This modification of the packing compared to the previous crystal (form-a) can be analyzed using the Hirshfeld surface components (Figure S12): in this case there are

stronger stacking interactions and also more directional C–H···Cl and C–H···F interactions, due to the coupling between inverted molecules.

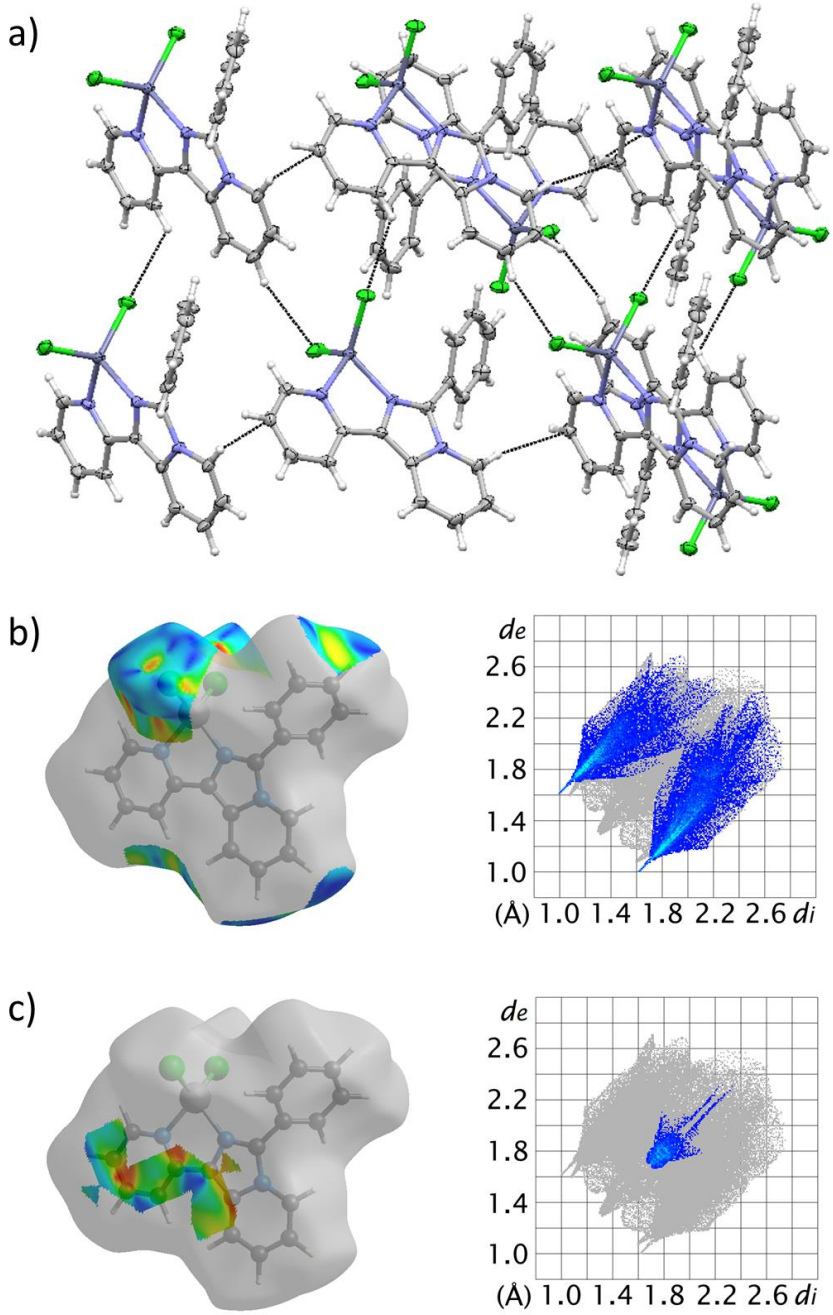

Figure 3. Packing plane formed by weak hydrogen bond interactions in the crystal structure of **Zn(L1)Cl$_2$** (a). (b) C–H···Cl and (c) π···π stacking regions on the Hirshfeld surface and in the decomposed fingerprint.

Complex **Zn(L3)Cl$_2$** crystallizes in the triclinic *P-1* space group with one molecule in the asymmetric unit. The geometry is similar to the previous ones, with a comparable dihedral angle between the central ligand core and the phenyl substituent, suggesting an analogous steric hindrance of the para substituent (although the *tert*-butyl substituent does not present the positional disorder observed in the **Zn(L2)Cl$_2$** crystals). The packing is a complex interplay of C–H···Cl between couples of stacked inverted dimers that form a 3D pattern and are reflected in the fingerprint of the molecule by longer stripes, if compared to the previously analyzed cases (Figure S14).

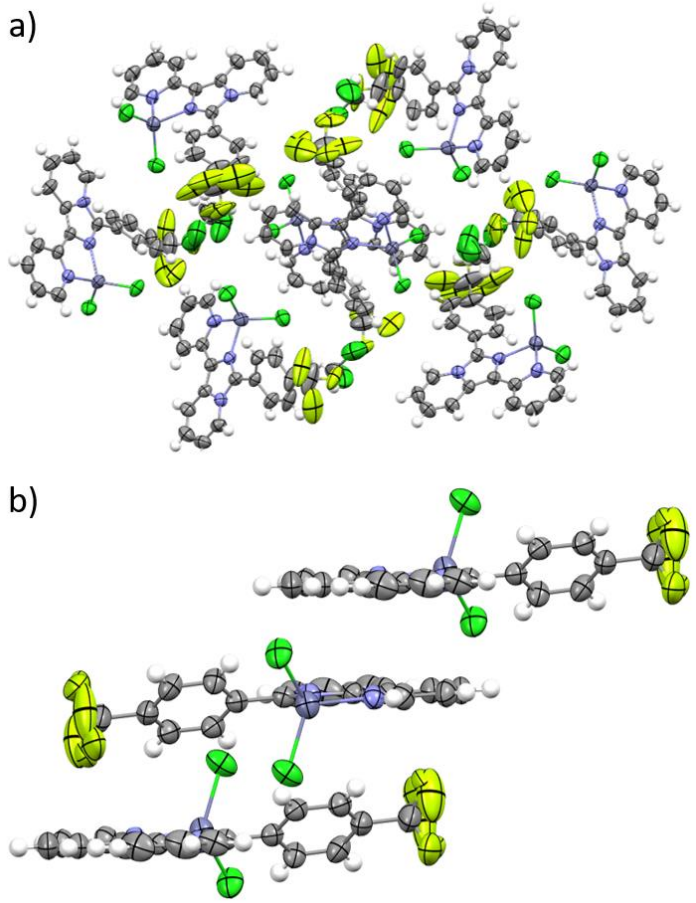

Figure 4. (a) Packing projection along a axis in form-a of **Zn(L2)Cl$_2$** and (b) (100) plane of molecules in form-b of **Zn(L2)Cl$_2$**.

By analyzing the crystal packing of the four crystals from a topological point of view (considering Van der Waals contacts as defining interactions), the underlying net of **Zn(L1)Cl$_2$** and **Zn(L3)Cl$_2$** crystals is a simple uninodal net with a molecular coordination number of 14 (calculated from Voronoj-Dirichlet polyhedron, Figures S15-S18), as usually found for molecular compounds (point symbol for the two cases: $\{3^{45}.4^{63}.5^{12}\}$ and $\{3^{45}.4^{68}.5^{7}\}$ respectively).[57,58] On the other hand, the peculiarity of form-a and form-b of **Zn(L2)Cl$_2$** is the underlying trinodal net with a smaller molecular coordination number for each node (point symbol for the two cases: $\{3^{4}.4^{6}.5^{5}\}\{3^{7}.4^{10}.5^{14}.6^{5}\}\{3^{7}.4^{9}.5^{5}\}$ and $\{3^{17}.4^{10}.5\}\{3^{2}.4\}\{3^{68}.4^{156}.5^{47}.6^{5}\}$ respectively). These results, calculated using ToposPro software[59] (complete data can be found in the supplementary material, Figures S19-S22), make clear the inherent difference between the inequivalent molecules in form-b and the peculiarities of Z' > 1 structures.

2.3 Mass Spectrometry

The ESI mass spectrum (positive ion mode) of **Zn(L1)Cl$_2$** is reported in Figure 5. The complex does not display free basic sites where cations usually present in the ESI environment (such as Na^+, K^+ or NH_4^+) may bind and impart a positive charge. As a consequence, neither the protonated molecular ion, $[M+H]^+$, nor the cationized adducts are present in the spectra. However, the loss of a chloride ligand yields the $[Zn(L1)Cl]^+$ ion, whose signal is detectable at *m/z* = 370; this signal provides indication of a 1:1 ligand-metal complexation ratio, as expected. The other peaks can be ascribed to

equilibria taking place in solution: free ligand protonation ($L1H^+$, *m/z* = 272) and addition of a ligand molecule to the $[Zn(L1)Cl]^+$ ion, yielding $[Zn(L1)_2Cl]^+$ (*m/z* = 641) which in turn originates $[Zn(L1)_2]^{2+}$ (*m/z* = 303) after the loss of the chloride. The presence of the doubly charged $[Zn(L1)_2]^{2+}$ ion was confirmed by high resolution experiments.

The mass spectra of complexes **Zn(L2)Cl$_2$** and **Zn(L3)Cl$_2$** (Figures S1 and S2, respectively) are very similar and do not show remarkable differences with respect to the one of **Zn(L1)Cl$_2$**. The main peak is due to the $[Zn(L)_2Cl]^+$ ion (*m/z* = 777, and *m/z* = 753). Protonated ligands $L2H^+$ (*m/z* = 340) and $L3H^+$ (*m/z* = 328), $[Zn(L)Cl]^+$ (*m/z* = 440 and *m/z* = 426), $[Zn(L)_2]^{2+}$ (*m/z* = 371 and *m/z* = 359) are the other main identified species in the spectra, which were already detected in the spectrum of **Zn(L1)Cl$_2$**. Moreover, a weak signal due to the $[Zn(L)_3]^{2+}$ ion (*m/z* = 540 and *m/z* = 523) is also present for these two complexes. Finally, the peaks at *m/z* = 914 (Figure S1) and 891 (Figure S2) were assigned to the $[Zn(L)_2Cl + ZnCl_2]^+$ adduct, which is a typical gas phase ion formed under ESI conditions. The experimental mass distributions for all the observed ions nicely fit with the calculated isotopic mass distributions, thus representing an additional proof for ion assignment.

Even if the absence of free basic sites in the complexes does not allow formation of cationized molecular ions, nevertheless the signals of the metal-ligand 1:1 complexes are present in the ESI spectra of each complex, while the other peaks are attributed to equilibria taking place in the environment of the ESI source. Moreover, elemental analysis and single-crystal X-ray diffraction leave no doubts about the 1:1 metal-to-ligand ratio for the synthesized complexes in the solid phase.

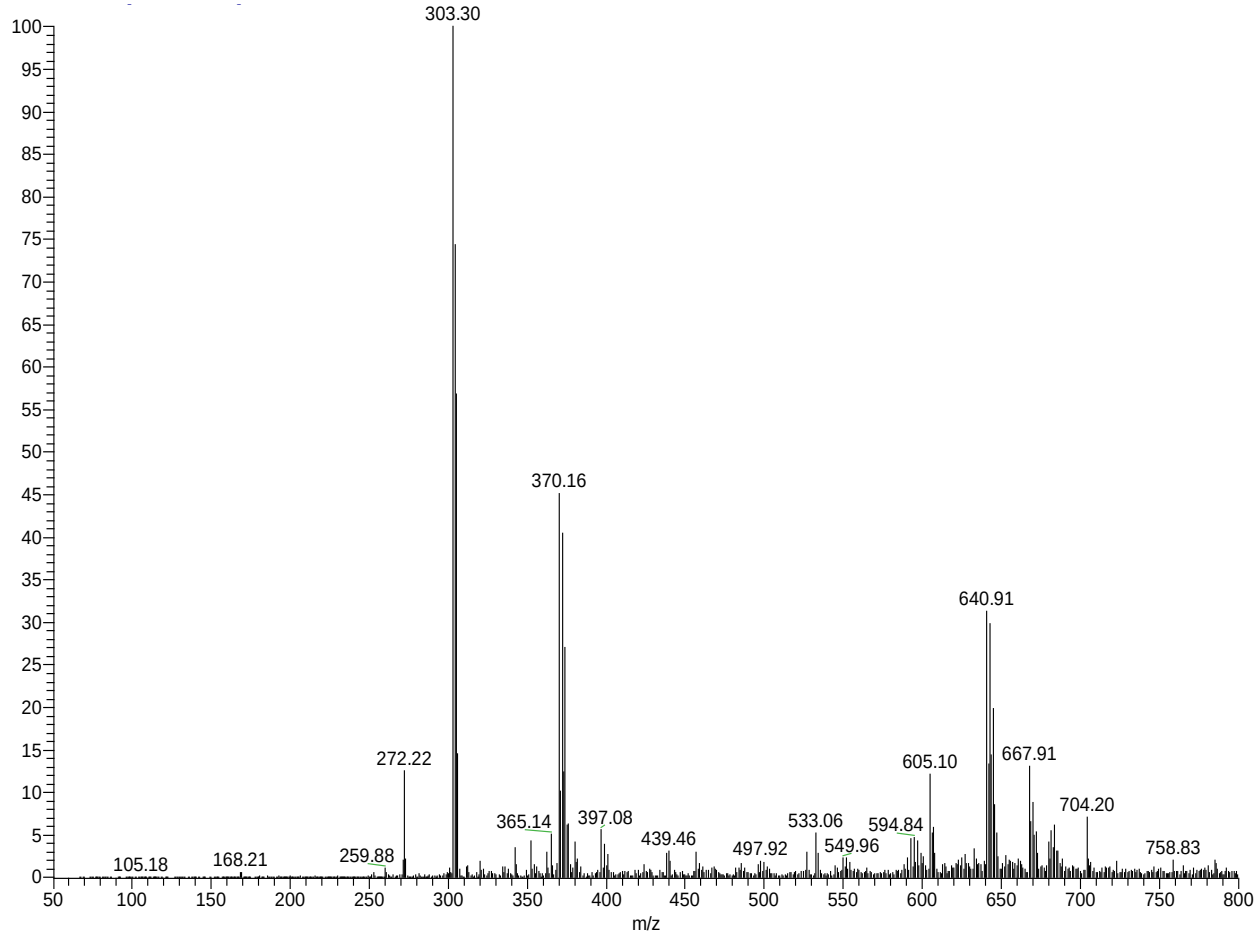

Figure 5. ESI mass spectrum of complex **Zn(L1)Cl$_2$**.

2.4 Vibrational characterization

Raman spectra of **Zn(L1)Cl$_2$**, **Zn(L2)Cl$_2$** and **Zn(L3)Cl$_2$** show the pattern of the corresponding ligand: signals are generally shifted to higher wavenumbers for the rigidity imposed by metal coordination (see Table 1 and Figure 6 and Figures S3 and S4). In particular the breathing mode of the pyridyl fragment, around 1000 cm^{-1}, has a shift of around 15 cm^{-1}, confirming the formation of the chelating ring.[60] Far infrared spectra were recorded to observe signals related to the metal center: in the spectra of the complexes there are two strong peaks absent in the spectra of the ligands. According to literature, these signals could be attributed to Zn–Cl stretching modes.[61]

Table 1. Raman and Far IR signals of ligands **L1**–**L3** and of the related Zn(L)Cl$_2$ complexes.

L1	**Zn(L1)Cl$_2$**	**L2**	**Zn(L2)Cl$_2$**	**L3**	**Zn(L3)Cl$_2$**	Assigment
1631 m	1638 w	1634 m	1642 w	1632 m	1640 w	
1602 s	1604 vs	1619 s	1621 s	1614 m	1609 m	
1588 s	1562 w	1588 s	1604 m	1588 s	1601 m	
1533 vs	1547 s	1565 w	1567 w	1563 w	1562 w	$\nu_{C—N}$, $\nu_{C—C}$
1523 s	1533 s	1538 s	1550 s	1538 s	1548 vs	
1507 vs	1513 vs	1512 vs	1541 s	1512 vs	1517 s	
			1519 vs			
980 s	994 s	983 m	997 w	983 m	994 m	
997 m	1012 m	996 w	1019 w	993 w	1017 m	$\nu_{C—C}$
	1023 m		1030 w		1026 w	
	331 s		336 s		332 s	$\nu_{Zn—Cl}$
	308 s		304 s		309 s	

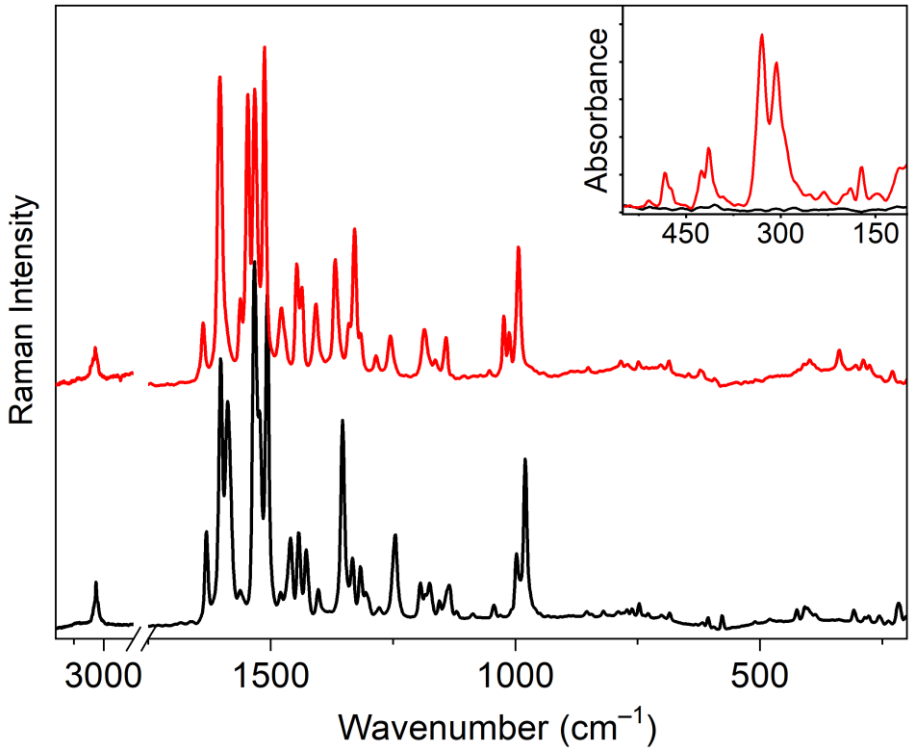

Figure 6. Raman and FIR (inset) spectra of **L1** (black) and **Zn(L1)Cl$_2$** (red).

2.5 Optical characterization

The optical data obtained for the free ligands, **L1**–**L3**, and for the corresponding complexes, **Zn(L1)Cl2**, **Zn(L2)Cl2**, **Zn(L3)Cl2**, in dichloromethane solution are collected in Table 2, while their absorption and emission spectra are presented in Figure 7 and Figure 8.

The free ligands show the main absorption features in the wavelength range between 280 nm and 380 nm, with almost no absorption beyond 400 nm. Each ligand shows one main peak in the 310–330 nm range and a shoulder (a second peak for **L2**) centered at 360–380 nm. The various substituents on the imidazo[1,5-*a*]pyridine ligands have a definite effect on the absorption bands, in particular **L2** shows an hyperchromic effect in the 360–380 nm region.

The corresponding metal complexes present three main absorptions. One in the 310–330 nm range, a second one centered at 350–360 nm and a third one at 370–380 nm with a final shoulder at 390–398 nm. Compounds **Zn(L1)Cl2**, **Zn(L2)Cl2**, **Zn(L3)Cl2** show a smaller red shift if compared to the corresponding free ligand, as if the various substituents had a reduced effect on the absorption bands of the complexes. From these data it is evident that both electron-donating and electron-withdrawing groups, on the phenyl substituent in position 3 of the imidazo[1,5-*a*]pyridine, have a definite and opposite effect on the absorption behavior in the 350–390 nm range.

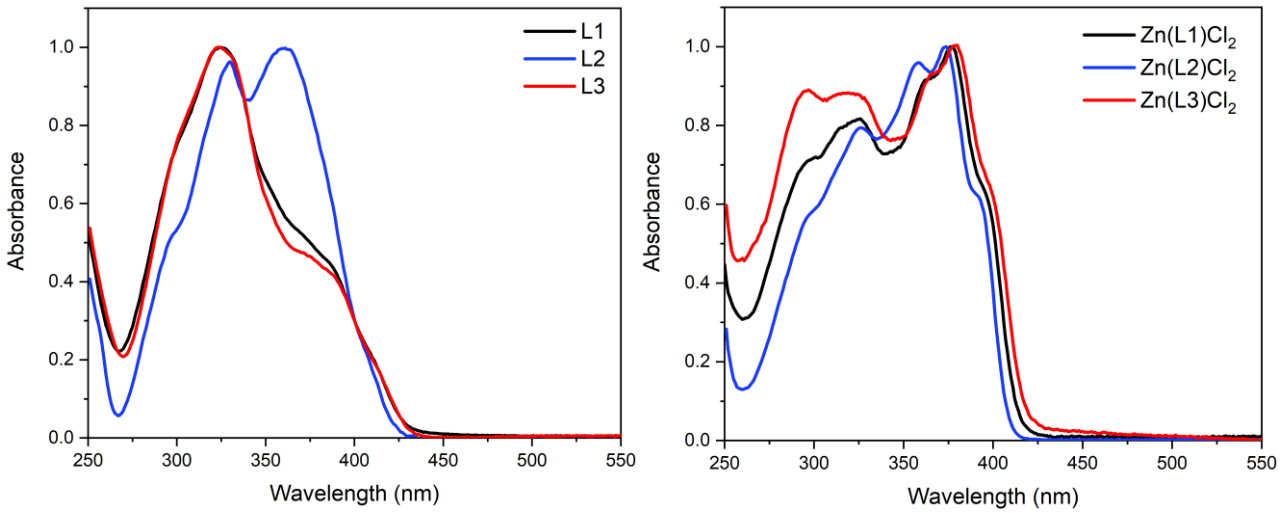

Figure 7. Normalized absorption spectra of **L1**–**L3** (left) and of the corresponding $Zn(L)Cl_2$ complexes (right).

The imidazo[1,5-*a*]pyridine nucleus is known in literature for its emissive properties[31,32,43,62–64]. The employed derivatives display an intense fluorescence emission centered at about 460 nm, characterized by quantum yields ranging from 15 to 21% in dichloromethane solutions. All the ligands show a large Stokes shift (80–140 nm).

The related complexes show similar emission profiles in dichloromethane solution. The luminescence is positioned in the blue region (430–450 nm) and is due to an intense intra-ligand (π–π*) transitions, as previously reported by us for similar system.[6,7,65] The emission spectrum consists of an intense structured band centered at about 440 nm and surrounded by two shoulders at 410–420 and 460–470 nm, more evident than for the free ligands.

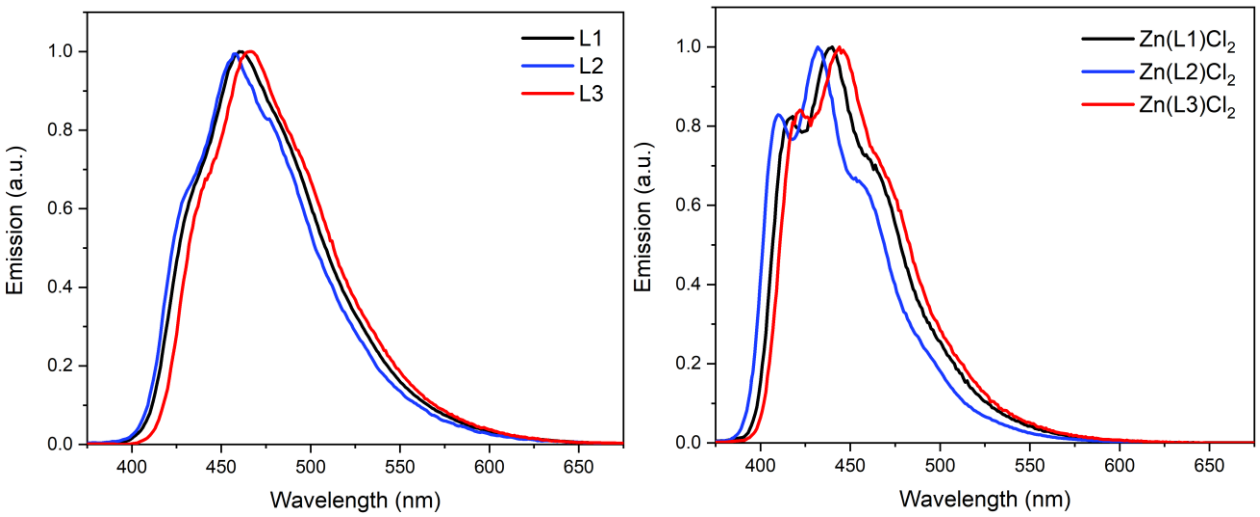

Figure 8. Emission spectra of ligand **L1**–**L3** (left) and of the corresponding $Zn(L)Cl_2$ complexes (right).

According to literature data, the emission maxima for zinc complexes with N,N-bidentate ligands (such as well known phenanthroline and bipyridine ligands) are generally red shifted of about 30–50 nm with respect to the free ligands.[6,66–68] Conversely, the $Zn(L)Cl_2$ complexes reported in this study display a remarkable hypsochromic shift (30–40 nm) if compared with the emission of the free imidazo[1,5-*a*]pyridine ligands. The strong blue-shift is related to the conformational modification of the ligand (from *trans* to *cis*) upon metal coordination. To the best of our knowledge, this interesting characteristic has never been observed in previous works on Zn(II) with analogous imidazo[1,5-*a*]pyridines. The hypsochromic shift of the emission, combined with the red shifted absorption, have as a consequence the reduction of the Stokes shift in the complexes, if compared with the corresponding free imidazo[1,5-*a*]pyridines. Moreover, comparing the $Zn(L)Cl_2$ complexes it is evident that the different substituents produce an opposite effect on the emission spectra.

Table 2. Absorption and emission data for **L1**–**L3** and for the corresponding complexes $Zn(L)Cl_2$.

Compound	Absorption (nm)	Emission (nm)	Stokes Shift (nm)	Quantum Yield (%)
L1	377sh 323	463	79	19
Zn(L1)Cl$_2$	395sh 376 362 325	416sh 440 462sh	64	32
L2	361 330	458	128	15
Zn(L2)Cl$_2$	373 358 325 392sh	410sh 431 458sh	57	33
L3	381sh 324	466	142	21
Zn(L3)Cl$_2$	398sh 380 365 324	422sh 445 470sh	64	31

In particular, **Zn(L2)Cl$_2$** results in the most hypsochromic shifted emission (431 nm), while **Zn(L3)Cl$_2$** has the most bathochromic one (445 nm). Predictable and significant changes in the emission maxima of the complexes have been obtained introducing electron-donating and electron-withdrawing substituents in the chemical structure of corresponding ligands.
A significant increase of the quantum yields results comparing the free ligands and the corresponding complexes. The values change from 19% (**L1**), 15% (**L2**) and 21% (**L3**), for the free ligands to 32%, 33% and 31% for the corresponding complexes, respectively. In particular, **Zn(L2)Cl$_2$** exhibits the maximum quantum yield (33%) which, to the best of our knowledge, is the highest reported in literature among the Zn(II) imidazo[1.5-a]pyridine complexes in solution.
This class of complexes is typically non sensitive to molecular oxygen, so that the emission from aerated solutions is not quenched. Indeed, in our case the emission profile and intensity of Zn(L)Cl$_2$ complexes in aerated and deaerated conditions are perfectly overlapped. The emission at λ = 410–460 nm is mainly LC (π–π*), in agreement with the vibrational profile of the band. Analogies with the corresponding Cu, Ir and Re derivatives are in agreement with this interpretation.[5–7,27,53,54,65] Furthermore, as can be seen from the emission spectra, no partial dissociation of the complexes was observed in dichloromethane solution, contrary to what previously reported in literature for analogue zinc complexes.[6] Indeed, the typical emission of the free ligands is not detectable in the solutions of the complexes.

3. Experimental

3.1 Material and methods

All solvents and raw materials were used as received from commercial suppliers (Sigma-Aldrich and Alfa Aesar) without further purification. TLC was performed on Fluka silica gel TLC-PET foils GF 254. particle size 25 nm. medium pore diameter 60 Å. Column chromatography was performed on Sigma-Aldrich silica gel 60 (70–230 mesh ASTM).
Mass spectra were recorded on a Thermo-Finnigan Advantage Max Ion Trap Spectrometer equipped with an electrospray ion source (ESI) in positive and negative ion acquiring mode.
UV-Vis absorption spectra were recorded on a Cary60 spectrometer. Photoemission spectra and luminescence quantum yields were acquired with a HORIBA Jobin Yvon IBH Fluorolog-TCSPC spectrofluorometer, equipped with a Quanta-φ integrating sphere. The spectral response was corrected for the spectral sensitivity of the photomultiplier.
Vibrational spectra were recorded for all products on powder samples. FT-Raman spectra were obtained with a Bruker Vertex 70 spectrometer, equipped with the RAM II accessory, by exciting with a 1064 nm laser, with a resolution of 4 cm^{-1}. FTIR spectra were obtained with the same instrument equipped with the Harrick MVP2 ATR cell and using a DTGS detector.
The elemental composition of the solid complexes was determined using a Thermo FlashEA 1112 CHNS–O analyser. Two replicas were performed, and values were presented as % mass mean value.
Zn(L)Cl$_2$ single crystals were analysed with a Gemini R Ultra diffractometer operating at 293(2) K, using a Mo−Kα source (λ = 0.71073 Å) (Cu-Kα source for the acetonitrile solvate of **Zn(L2)Cl$_2$**, form-b, λ = 1.54060 Å, for the small size of the crystal obtained). Data collection and reduction were performed using the CrysAlisPro software. The crystal structure was solved by direct methods and refined with the full matrix least-squares technique on F^2 using the SHELXS-97[69] and SHELXL-97[70] programs. All non-hydrogen atoms were refined anisotropically; hydrogen atoms were placed

in geometrical positions and refined using the riding model. Visualization of crystal structures has been performed using Mercury.[71] All the crystallographic and structural data can be consulted in the supplementary material. Topological analysis of all crystal structure has been done using ToposPro[72] and can be found in the supplementary material. The Hirshfeld surface analysis has been performed using CrystalMaker17[73] and can be found in the supplementary material. In $Zn(L2)Cl_2$ form-a and $Zn(L2)Cl_2$ form-b the $-CF_3$ disordered groups and solvent disorders have been modeled in the Hirshfeld surface calculation using the new cycling option of CrystalMaker17. This option includes all orientations of the disordered molecule with their partial occupancies and results in a Hirshfeld surface based on the smeared electron distribution based on the average structure with electron densities weighted by their partial occupancies.

The crystallographic data for **Zn(L1)Cl2**, **Zn(L2)Cl2**, and **Zn(L3)Cl2** have been deposited within the Cambridge Crystallographic Data Centre as supplementary publications, under the CCDC numbers 1947720-1947723. This information can be obtained free of charge from the Cambridge Crystallographic Data Centre via www.ccdc.cam.ac.uk/data_request/cifcode CCDC.

3.2 Syntheses

General procedure for 1,3-substituted-imidazo[1,5-*a*]pyridines (**L1**–**L3**).

Compounds **L1–L3** were prepared as previously reported.[27,53,54,74] Di(2-pyridyl)ketone (800 mg, 4.37 mmol, 1 eq), corresponding aldehyde (6.55 mmol, 1.5 eq.) and ammonium acetate (1704 mg, 21.85 mmol, 5 eq) in glacial acetic acid (25 mL). Reaction time: 5 h at 118 °C. The acetic acid was removed by evaporation under reduced pressure. The obtained solid was dissolved in a saturated aqueous solution of Na_2CO_3 and the mixture extracted with CH_2Cl_2. The organic layer was separated, dried and the solvent evaporated under vacuum. The obtained crude product was purified via column chromatography on silica gel (CH_2Cl_2-CH_3OH 98:2) and the product isolated as a yellowish solid.

Synthesis of $Zn(L)Cl_2$ complexes. To a suspension of $ZnCl_2$ (55 mg, 0.400 mmol) in methanol (15 ml) **L1**–**L3** (0.48 mmol, 1.2 eq.) was added, and a yellow suspension immediately formed. The suspension was stirred at room temperature for 2.5 h and then filtered; the yellow powder obtained in quantitative yield was washed with diethyl ether three times and dried under vacuum.

Zn(L1)Cl2 elemental analysis ($C_{18}H_{13}N_3Cl_2Zn$) – Theoretical: C = 53.04%, H = 3.21%, N = 10.31%; experimental: C = 53.34%, H = 3.17%, N = 10.17%.

Zn(L2)Cl2 elemental analysis ($C_{19}H_{12}N_3F_3Cl_2Zn$) – Theoretical: C = 47.98%, H = 2.54%, N = 8.84%; experimental: C = 47.65%, H = 2.46%, N = 8.51%.

Zn(L3)Cl2 elemental analysis ($C_{22}H_{21}N_3Cl_2Zn$) – Theoretical: C = 56.68%, H = 4.56%, N = 9.06%; experimental: C = 56.35%, H = 4.36%, N = 8.69%.

4. Conclusions

Three new fluorescent 1,3-substituted-imidazo[1,5-*a*]pyridine zinc(II) chlorido complexes have been synthesized, structurally and electronically characterized. The luminescent imidazo[1,5-*a*]pyridine core, usefully substituted in position 3 with phenyl group (**L1**) or electron-donating (trifluoromethyl group **L2**) and electron-withdrawing pendant group (*tert*-butyl group **L3**) on the phenyl, have been employed to obtain the corresponding Zn(II) complexes in high yields.

The structure of the achieved compounds has been determined by single-crystal X-ray diffraction, optical and vibrational spectroscopy, electrospray ionization mass spectrometry and elemental analysis. The comparison of the photophysical properties, induced by the modification of the

substituent on the imidazo[1,5-*a*]pyridine ligands, led us throughout the synthesis of the corresponding Zn(II) chlorido complexes. The obtained optical properties of the $ZnLCl_2$ products demonstrate a suitable optical tunability, related to the chemical structure, and an intense increase of the quantum yield after complexation. Electronic absorption and emission spectra of the compounds have been investigated in dichloromethane, showing for the first time a surprising hypsochromic shift (30-40 nm) in spectra of the Zn(II) complexes if compared with the emission of the free ligands, on the contrary to what reported in the literature for other N,N-bidentate ligands (such as well know phenanthroline and bipyridine). In general, the obtained 1,3-substituted-imidazo[1,5-*a*]pyridine complexes show absorption maxima below 410 nm, with a suitable transparency in the visible range, and a powerful emissions in the blue region (430-445 nm).
On the basis of these promising properties further studies are in progress to test these products as tunable low-cost emitting materials for possible and desirable technological applications.

Funding

This research did not receive any specific grant from funding agencies in the public, commercial, or not-for-profit sectors.

References

[1] O. Veselska, A. Demessence, d10 coinage metal organic chalcogenolates: From oligomers to coordination polymers, Coord. Chem. Rev. 355 (2018) 240–270. https://doi.org/10.1016/j.ccr.2017.08.014.

[2] J. Schaefer, A. Kraft, S. Reininger, G. Santiso-Quinones, D. Himmel, N. Trapp, U. Gellrich, B. Breit, I. Krossing, A Systematic Investigation of Coinage Metal Carbonyl Complexes Stabilized by Fluorinated Alkoxy Aluminates, Chem. – Eur. J. 19 (2013) 12468–12485. https://doi.org/10.1002/chem.201204544.

[3] G. Cheng, G.K.-M. So, W.-P. To, Y. Chen, C.-C. Kwok, C. Ma, X. Guan, X. Chang, W.-M. Kwok, C.-M. Che, Luminescent zinc(II) and copper(I) complexes for high-performance solution-processed monochromic and white organic light-emitting devices, Chem. Sci. 6 (2015) 4623–4635. https://doi.org/10.1039/C4SC03161J.

[4] E. Fresta, G. Volpi, M. Milanesio, C. Garino, C. Barolo, R.D. Costa, Novel Ligand and Device Designs for Stable Light-Emitting Electrochemical Cells Based on Heteroleptic Copper(I) Complexes, Inorg. Chem. 57 (2018) 10469–10479. https://doi.org/10.1021/acs.inorgchem.8b01914.

[5] E. Fresta, G. Volpi, C. Garino, C. Barolo, R.D. Costa, Contextualizing yellow light-emitting electrochemical cells based on a blue-emitting imidazo-pyridine emitter, Polyhedron. 140 (2018) 129–137. https://doi.org/10.1016/j.poly.2017.11.048.

[6] G.A. Ardizzoia, S. Brenna, S. Durini, B. Therrien, Synthesis and characterization of luminescent zinc(II) complexes with a N,N-bidentate 1-pyridylimidazo[1,5-a]pyridine ligand, Polyhedron. 90 (2015) 214–220. https://doi.org/10.1016/j.poly.2015.02.005.

[7] G.A. Ardizzoia, S. Brenna, S. Durini, B. Therrien, M. Veronelli, Synthesis, Structure, and Photophysical Properties of Blue-Emitting Zinc(II) Complexes with 3-Aryl-Substituted 1-Pyridylimidazo[1,5-a]pyridine Ligands, Eur. J. Inorg. Chem. (2014) 4310–4319. https://doi.org/10.1002/ejic.201402415.

[8] C. Seward, J. Pang, S. Wang, Luminescent star-shaped zinc(II) and platinum(II) complexes based on star-shaped 2,2 ’-dipyridylamino-derived ligands, Eur. J. Inorg. Chem. 2002 (2002) 1390–1399. https://doi.org/10.1002/1099-0682(200206)2002:6<1390::AID-EJIC1390>3.0.CO;2-E.

[9] M. Srinivas, G.R. Vijayakumar, K.M. Mahadevan, H. Nagabhushana, H.S. Bhojya Naik, Synthesis, photoluminescence and forensic applications of blue light emitting azomethine-zinc (II) complexes of bis(salicylidene)cyclohexyl-1,2-diamino based organic ligands, J. Sci. Adv. Mater. Devices. 2 (2017) 156–164. https://doi.org/10.1016/j.jsamd.2017.02.008.

[10] Y. Sakai, Y. Sagara, H. Nomura, N. Nakamura, Y. Suzuki, H. Miyazaki, C. Adachi, Zinc complexes exhibiting highly efficient thermally activated delayed fluorescence and their application to organic light-emitting diodes, Chem. Commun. 51 (2015) 3181–3184. https://doi.org/10.1039/C4CC09403D.
[11] F. Dumur, Zinc complexes in OLEDs: An overview, Synth. Met. 195 (2014) 241–251. https://doi.org/10.1016/j.synthmet.2014.06.018.
[12] R. Pandey, P. Kumar, A.K. Singh, M. Shahid, P. Li, S.K. Singh, Q. Xu, A. Misra, D.S. Pandey, Fluorescent Zinc(II) Complex Exhibiting "On-Off-On" Switching Toward Cu2+ and Ag+ Ions, Inorg. Chem. 50 (2011) 3189–3197. https://doi.org/10.1021/ic1018086.
[13] A. Barbieri, G. Accorsi, N. Armaroli, Luminescent complexes beyond the platinum group: the d10 avenue, Chem. Commun. (2008) 2185–2193. https://doi.org/10.1039/B716650H.
[14] E. Priola, G. Volpi, R. Rabezzana, E. Borfecchia, C. Garino, P. Benzi, A. Martini, L. Operti, E. Diana, Bridging Solution and Solid-State Chemistry of Dicyanoaurate: The Case Study of Zn–Au Nucleation Units, Inorg. Chem. 59 (2020) 203–213. https://doi.org/10.1021/acs.inorgchem.9b00961.
[15] A. Herbst, C. Bronner, P. Dechambenoit, O.S. Wenger, Gold Complexes with Tridentate Cyclometalating and NHC Ligands: A Search for New Photoluminescent Gold(III) Compounds, Organometallics. 32 (2013) 1807–1814. https://doi.org/10.1021/om301226b.
[16] G. Cui, X.-Y. Cao, W.-H. Fang, M. Dolg, W. Thiel, Photoinduced Gold(I)–Gold(I) Chemical Bonding in Dicyanoaurate Oligomers, Angew. Chem. Int. Ed. 52 (2013) 10281–10285. https://doi.org/10.1002/anie.201305487.
[17] K. Li, G.S.M. Tong, Q. Wan, G. Cheng, W.-Y. Tong, W.-H. Ang, W.-L. Kwong, C.-M. Che, Highly phosphorescent platinum(II) emitters: photophysics, materials and biological applications, Chem. Sci. 7 (2016) 1653–1673. https://doi.org/10.1039/C5SC03766B.
[18] A.Y.Y. Tam, D.P.K. Tsang, M.Y. Chan, N.Y. Zhu, V.W.W. Yam, A luminescent cyclometalated platinum(II) complex and its green organic light emitting device with high device performance, Chem. Commun. 47 (2011) 3383–3385. https://doi.org/10.1039/C0CC05538G.
[19] W.Y. Wong, C.L. Ho, Heavy metal organometallic electrophosphors derived from multi-component chromophores, Coord. Chem. Rev. 253 (2009) 1709–1758. https://doi.org/10.1016/j.ccr.2009.01.013.
[20] C. Coluccini, N. Manfredi, M.M. Salamone, R. Ruffo, M.G. Lobello, F. De Angelis, A. Abbotto, Quaterpyridine Ligands for Panchromatic Ru(II) Dye Sensitizers, J. Org. Chem. 77 (2012) 7945–7956. https://doi.org/10.1021/jo301226z.
[21] M. Janghouri, White-light-emitting devices based on Nile Red and π electron rich [Zn4core] complex, Opt. Quantum Electron. 49 (2017) 410. https://doi.org/10.1007/s11082-017-1250-x.
[22] H. Li, F. Zhang, Y. Wang, D. Zheng, Synthesis and characterization of tris-(8-hydroxyquinoline)aluminum, Mater. Sci. Eng. B. 100 (2003) 40–46. https://doi.org/10.1016/S0921-5107(03)00067-9.
[23] Y. Chen, L. Li, Z. Chen, Y. Liu, H. Hu, W. Chen, W. Liu, Y. Li, T. Lei, Y. Cao, Z. Kang, M. Lin, W. Li, Metal-Mediated Controllable Creation of Secondary, Tertiary, and Quaternary Carbon Centers: A Powerful Strategy for the Synthesis of Iron, Cobalt, and Copper Complexes with in Situ Generated Substituted 1-Pyridineimidazo[1,5-a]pyridine Ligands, Inorg. Chem. 51 (2012) 9705–9713. https://doi.org/10.1021/ic300949y.
[24] N. Kundu, S.M.T. Abtab, S. Kundu, A. Endo, S.J. Teat, M. Chaudhury, Triple-Stranded Helicates of Zinc(II) and Cadmium(II) Involving a New Redox-Active Multiring Nitrogenous Heterocyclic Ligand: Synthesis, Structure, and Electrochemical and Photophysical Properties, Inorg. Chem. 51 (2012) 2652–2661. https://doi.org/10.1021/ic202595p.
[25] Y. Chen, L. Li, Y. Cao, J. Wu, Q. Gao, Y. Li, H. Hu, W. Liu, Y. Liu, Z. Kang, J. Li, Cu-II-mediated controllable creation of tertiary and quaternary carbon centers: designed assembly and structures of a new class of copper complexes supported by in situ generated substituted 1-pyridineimidazo[1,5-a]pyridine ligands, Crystengcomm. 15 (2013) 2675–2681. https://doi.org/10.1039/c3ce00012e.
[26] E. Baranoff, S. Fantacci, F. De Angelis, X.X. Zhang, R. Scopelliti, M. Gratzel, M.K. Nazeeruddin, Cyclometalated Iridium(III) Complexes Based on Phenyl-Imidazole Ligand, Inorg. Chem. 50 (2011) 451–462. https://doi.org/10.1021/ic901834v.

[27] C. Garino, T. Ruiu, L. Salassa, A. Albertino, G. Volpi, C. Nervi, R. Gobetto, K.I. Hardcastle, Spectroscopic and computational study on new blue emitting ReL(CO)(3)Cl complexes containing pyridylimidazo[1,5-a]pyridine ligands, Eur. J. Inorg. Chem. (2008) 3587–3591. https://doi.org/10.1002/ejic.200800348.
[28] S. Durini, G.A. Ardizzoia, B. Therrien, S. Brenna, Tuning the fluorescence emission in mononuclear heteroleptic trigonal silver(I) complexes, New J. Chem. 41 (2017) 3006–3014. https://doi.org/10.1039/C6NJ04058F.
[29] G. Albrecht, C. Geis, J.M. Herr, J. Ruhl, R. Göttlich, D. Schlettwein, Electroluminescence and contact formation of 1-(pyridin-2-yl)-3-(quinolin-2-yl)imidazo[1,5-a]quinoline thin films, Org. Electron. 65 (2019) 321–326. https://doi.org/10.1016/j.orgel.2018.11.032.
[30] J.T. Hutt, J. Jo, A. Olasz, C.-H. Chen, D. Lee, Z.D. Aron, Fluorescence Switching of Imidazo[1,5-a]pyridinium Ions: pH-Sensors with Dual Emission Pathways, Org. Lett. 14 (2012) 3162–3165. https://doi.org/10.1021/ol3012524.
[31] G. Volpi, C. Garino, E. Conterosito, C. Barolo, R. Gobetto, G. Viscardi, Facile synthesis of novel blue light and large Stoke shift emitting tetradentate polyazines based on imidazo[1,5-a]pyridine, Dyes Pigments. 128 (2016) 96–100. https://doi.org/10.1016/j.dyepig.2015.12.005.
[32] G. Volpi, C. Garino, E. Priola, E. Diana, R. Gobetto, R. Buscaino, G. Viscardi, C. Barolo, Facile synthesis of novel blue light and large Stoke shift emitting tetradentate polyazines based on imidazo[1,5-a]pyridine – Part 2, Dyes Pigments. 143 (2017) 284–290. https://doi.org/10.1016/j.dyepig.2017.04.034.
[33] J. Hu, Y. Li, Y. Wu, W. Liu, Y. Wang, Y. Li, Syntheses and Optical Properties of BODIPY Derivatives Based on Imidazo[1,5-a]pyridine, Chem. Lett. 44 (2015) 645–647. https://doi.org/10.1246/cl.150133.
[34] E. Yamaguchi, F. Shibahara, T. Murai, 1-Alkynyl- and 1-Alkenyl-3-arylimidazo[1,5-a]pyridines: Synthesis, Photophysical Properties, and Observation of a Linear Correlation between the Fluorescent Wavelength and Hammett Substituent Constants, J. Org. Chem. 76 (2011) 6146–6158. https://doi.org/10.1021/jo200864x.
[35] F. Shibahara, A. Kitagawa, E. Yamaguchi, T. Murai, Synthesis of 2-azaindolizines by using an iodine-mediated oxidative desulfurization promoted cyclization of N-2-pyridylmethyl thioamides and an investigation of their photophysical properties, Org. Lett. 8 (2006) 5621–5624. https://doi.org/10.1021/ol0623623.
[36] G. Volpi, G. Magnano, I. Benesperi, D. Saccone, E. Priola, V. Gianotti, M. Milanesio, E. Conterosito, C. Barolo, G. Viscardi, One pot synthesis of low cost emitters with large Stokes' shift, Dyes Pigments. 137 (2017) 152–164. https://doi.org/10.1016/j.dyepig.2016.09.056.
[37] G. Volpi, C. Magistris, C. Garino, Natural aldehyde extraction and direct preparation of new blue light-emitting imidazo[1,5-a]pyridine fluorophores, Nat. Prod. Res. 32 (2018) 2304–2311. https://doi.org/10.1080/14786419.2017.1410803.
[38] J.T. Hutt, Z.D. Aron, Synthesis and Application of Ratiometric and "Turn-On" Fluorescent pH Sensors: An Advanced Organic Undergraduate Laboratory, J. Chem. Educ. 91 (2014) 1990–1994. https://doi.org/10.1021/ed4006166.
[39] Y. Ge, R. Ji, S. Shen, X. Cao, F. Li, A ratiometric fluorescent probe for sensing Cu2+ based on new imidazo[1,5-a]pyridine fluorescent dye, Sens. Actuators B Chem. 245 (2017) 875–881. https://doi.org/10.1016/j.snb.2017.01.169.
[40] D.R. Mohbiya, N. Sekar, Tuning 'Stokes Shift' and ICT Character by Varying the Donor Group in Imidazo[1,5 a]pyridines: A Combined Optical, DFT, TD-DFT and NLO Approach, ChemistrySelect. 3 (2018) 1635–1644. https://doi.org/10.1002/slct.201702579.
[41] G. Volpi, C. Garino, E. Priola, C. Magistris, M.R. Chierotti, C. Barolo, Halogenated imidazo[1,5-a]pyridines: chemical structure and optical properties of a promising luminescent scaffold, Dyes Pigments. 171 (2019) 107713. https://doi.org/10.1016/j.dyepig.2019.107713.
[42] M. Roy, B.V.S.K. Chakravarthi, C. Jayabaskaran, A.A. Karande, A.R. Chakravarty, Impact of metal binding on the antitumor activity and cellular imaging of a metal chelator cationic imidazopyridine derivative, Dalton Trans. 40 (2011) 4855–4864. https://doi.org/10.1039/C0DT01717E.
[43] G. Volpi, B. Lace, C. Garino, E. Priola, E. Artuso, P. Cerreia Vioglio, C. Barolo, A. Fin, A. Genre, C. Prandi, New substituted imidazo[1,5-a]pyridine and imidazo[5,1-a]isoquinoline derivatives and their

application in fluorescence cell imaging, Dyes Pigments. 157 (2018) 298–304. https://doi.org/10.1016/j.dyepig.2018.04.037.
[44] F. Yagishita, C. Nii, Y. Tezuka, A. Tabata, H. Nagamune, N. Uemura, Y. Yoshida, T. Mino, M. Sakamoto, Y. Kawamura, Fluorescent N-Heteroarenes Having Large Stokes Shift and Water Solubility Suitable for Bioimaging, Asian J. Org. Chem. 7 (2018) 1614–1619. https://doi.org/10.1002/ajoc.201800250.
[45] Y. Ren, L. Zhang, Z. Zhou, Y. Luo, S. Wang, S. Yuan, Y. Gu, Y. Xu, X. Zha, A new lysosome-targetable fluorescent probe with a large Stokes shift for detection of endogenous hydrogen polysulfides in living cells, Anal. Chim. Acta. 1056 (2019) 117–124. https://doi.org/10.1016/j.aca.2018.12.051.
[46] G.-J. Song, S.-Y. Bai, X. Dai, X.-Q. Cao, B.-X. Zhao, A ratiometric lysosomal pH probe based on the imidazo[1,5-a]pyridine-rhodamine FRET and ICT system, Rsc Adv. 6 (2016) 41317–41322. https://doi.org/10.1039/c5ra25947a.
[47] D. Davey, P.W. Erhardt, W.C. Lumma, J. Wiggins, M. Sullivan, D. Pang, E. Cantor, Cardiotonic Agents .1. Novel 8-Aryl-Substituted Imidazo[1,2-a] and [1,5-a]Pyridines and Imidazo[1,5-a]Pyridinones as Potential Positive Inotropic Agents, J. Med. Chem. 30 (1987) 1337–1342.
[48] N.F. Ford, L.J. Browne, T. Campbell, C. Gemenden, R. Goldstein, C. Gude, J.W.F. Wasley, Imidazo[1,5-a]Pyridines - a New Class of Thromboxane-A2 Synthetase Inhibitors, J. Med. Chem. 28 (1985) 164–170.
[49] B.P. Fauber, A. Gobbi, K. Robarge, A. Zhou, A. Barnard, J. Cao, Y. Deng, C. Eidenschenk, C. Everett, A. Ganguli, J. Hawkins, A.R. Johnson, H. La, M. Norman, G. Salmon, S. Summerhill, W. Ouyang, W. Tang, H. Wong, Discovery of imidazo[1,5-a]pyridines and -pyrimidines as potent and selective RORc inverse agonists, Bioorg. Med. Chem. Lett. 25 (2015) 2907–2912. https://doi.org/10.1016/j.bmcl.2015.05.055.
[50] S. Priyanga, T. Khamrang, M. Velusamy, S. Karthi, B. Ashokkumar, R. Mayilmurugan, Coordination geometry-induced optical imaging of L-cysteine in cancer cells using imidazopyridine-based copper(II) complexes, Dalton Trans. 48 (2019) 1489–1503. https://doi.org/10.1039/C8DT04634D.
[51] M.A. Ingersoll, A.S. Lyons, S. Muniyan, N. D'Cunha, T. Robinson, K. Hoelting, J.G. Dwyer, X.R. Bu, S.K. Batra, M.-F. Lin, Novel Imidazopyridine Derivatives Possess Anti-Tumor Effect on Human Castration-Resistant Prostate Cancer Cells, PLOS ONE. 10 (2015) e0131811. https://doi.org/10.1371/journal.pone.0131811.
[52] A.M. Blanco-Rodríguez, H. Kvapilova, J. Sykora, M. Towrie, C. Nervi, G. Volpi, S. Zalis, A. Vlcek, Photophysics of Singlet and Triplet Intraligand Excited States in [ReCl(CO)3(1-(2-pyridyl)-imidazo[1,5-α]pyridine)] Complexes, J. Am. Chem. Soc. 136 (2014) 5963–5973. https://doi.org/10.1021/ja413098m.
[53] G. Volpi, C. Garino, L. Salassa, J. Fiedler, K.I. Hardcastle, R. Gobetto, C. Nervi, Cationic Heteroleptic Cyclometalated Iridium Complexes with 1-Pyridylimidazo[1,5-alpha]pyridine Ligands: Exploitation of an Efficient Intersystem Crossing, Chem.- Eur. J. 15 (2009) 6415–6427. https://doi.org/10.1002/chem.200801474.
[54] L. Salassa, C. Garino, A. Albertino, G. Volpi, C. Nervi, R. Gobetto, K.I. Hardcastle, Computational and spectroscopic studies of new rhenium(I) complexes containing pyridylimidazo[1,5-a]pyridine ligands: Charge transfer and dual emission by fine-tuning of excited states, Organometallics. 27 (2008) 1427–1435. https://doi.org/10.1021/om701175z.
[55] G.R. Desiraju, On the presence of multiple molecules in the crystal asymmetric unit (Z' > 1), CrystEngComm. 9 (2006) 91–92. https://doi.org/10.1039/B614933B.
[56] L. Yang, D.R. Powell, R.P. Houser, Structural variation in copper(I) complexes with pyridylmethylamide ligands: structural analysis with a new four-coordinate geometry index, τ4, Dalton Trans. (2007) 955–964. https://doi.org/10.1039/B617136B.
[57] E.V. Peresypkina, V.A. Blatov, Molecular coordination numbers in crystal -structures of organic compounds, Acta Crystallogr. B. 56 (2000) 501–511. https://doi.org/10.1107/S0108768199016675.
[58] E.V. Peresypkina, V.A. Blatov, Topology of molecular packings in organic crystals, Acta Crystallogr. B. 56 (2000) 1035–1045. https://doi.org/10.1107/S0108768100011824.
[59] M. Li, D. Li, M. O'Keeffe, O.M. Yaghi, Topological Analysis of Metal–Organic Frameworks with Polytopic Linkers and/or Multiple Building Units and the Minimal Transitivity Principle, Chem. Rev. 114 (2014) 1343–1370. https://doi.org/10.1021/cr400392k.

[60] A.E. Ozel, S. Kecel, S. Akyuz, Vibrational analysis and quantum chemical calculations of 2,2'-bipyridine Zinc(II) halide complexes, J. Mol. Struct. 834–836 (2007) 548–554. https://doi.org/10.1016/j.molstruc.2006.12.045.
[61] C. Postmus, J.R. Ferraro, W. Woznizk, Low-frequency infrared spectra of nitrogen-ligand complexes of zinc(II) halides, Inorg. Chem. 6 (1967) 2030–2032. https://doi.org/10.1021/ic50057a021.
[62] Y.-Q. Ge, T. Wang, G.Y. Duan, L.H. Dong, X.Q. Cao, J.W. Wang, Synthesis, Characterization, Optical Properties and Theoretical Studies of Novel Substituted Imidazo[1,5-a]pyridinyl 1,3,4-Oxadiazole Derivatives, J. Fluoresc. 22 (2012) 1531–1538. https://doi.org/10.1007/s10895-012-1091-8.
[63] G. Volpi, C. Magistris, C. Garino, FLUO-SPICES: natural aldehydes extraction and one-pot reaction to prepare and characterize new interesting fluorophores, Educ. Chem. Eng. 24 (2018) 1–6. https://doi.org/10.1016/j.ece.2018.06.002.
[64] X. Zhang, G.-J. Song, X.-J. Cao, J.-T. Liu, M.-Y. Chen, X.-Q. Cao, B.-X. Zhao, A new fluorescent pH probe for acidic conditions, Rsc Adv. 5 (2015) 89827–89832. https://doi.org/10.1039/c5ra14174e.
[65] M.D. Weber, C. Garino, G. Volpi, E. Casamassa, M. Milanesio, C. Barolo, R.D. Costa, Origin of a counterintuitive yellow light-emitting electrochemical cell based on a blue-emitting heteroleptic copper(I) complex, Dalton Trans. 45 (2016) 8984–8993. https://doi.org/10.1039/C6DT00970K.
[66] A.H. Younes, L. Zhang, R.J. Clark, L. Zhu, Fluorescence of 5-Arylvinyl-5'-Methyl-2,2'-Bipyridyl Ligands and Their Zinc Complexes, J. Org. Chem. 74 (2009) 8761–8772. https://doi.org/10.1021/jo901889y.
[67] V.N. Kozhevnikov, O.V. Shabunina, D.S. Kopchuk, M.M. Ustinova, B. König, D.N. Kozhevnikov, Facile synthesis of 6-aryl-3-pyridyl-1,2,4-triazines as a key step toward highly fluorescent 5-substituted bipyridines and their Zn(II) and Ru(II) complexes, Tetrahedron. 64 (2008) 8963–8973. https://doi.org/10.1016/j.tet.2008.06.040.
[68] D.N. Kozhevnikov, O.V. Shabunina, D.S. Kopchuk, P.A. Slepukhin, V.N. Kozhevnikov, 5-Aryl-2,2'-bipyridines as tunable fluorophores, Tetrahedron Lett. 47 (2006) 7025–7029. https://doi.org/10.1016/j.tetlet.2006.07.111.
[69] G.M. Sheldrick, A short history of SHELX, Acta Crystallogr. Sect. A. 64 (2008) 112–122.
[70] G.M. Sheldrick, SHELXT – Integrated space-group and crystal-structure determination, Acta Crystallogr. Sect. Found. Adv. 71 (2015) 3–8. https://doi.org/10.1107/S2053273314026370.
[71] C.F. Macrae, P.R. Edgington, P. McCabe, E. Pidcock, G.P. Shields, R. Taylor, M. Towler, J. van De Streek, Mercury: visualization and analysis of crystal structures, J. Appl. Crystallogr. 39 (2006) 453–457. https://doi.org/10.1107/S002188980600731X.
[72] V.A. Blatov, A.P. Shevchenko, D.M. Proserpio, Applied Topological Analysis of Crystal Structures with the Program Package ToposPro, Cryst. Growth Des. 14 (2014) 3576–3586. https://doi.org/10.1021/cg500498k.
[73] C.F. Mackenzie, P.R. Spackman, D. Jayatilaka, M.A. Spackman, CrystalExplorer model energies and energy frameworks: extension to metal coordination compounds, organic salts, solvates and open-shell systems, IUCrJ. 4 (2017) 575–587. https://doi.org/10.1107/S205225251700848X.
[74] J. Wang, R. Mason, D. VanDerveer, K. Feng, X.R. Bu, Convenient preparation of a novel class of imidazo[1,5-a]pyridines: Decisive role by ammonium acetate in chemoselectivity, J. Org. Chem. 68 (2003) 5415–5418. https://doi.org/10.1021/jo0342020.